Bistability in microcavities with incoherent optical or electrical excitation

O. Kyriienko,[1,2] E. A. Ostrovskaya,[3] O. A. Egorov,[4] I. A. Shelykh,[1,2] and T. C. H. Liew[2]
[1]*Science Institute, University of Iceland, Dunhagi-3, IS-107, Reykjavik, Iceland*
[2]*Division of Physics and Applied Physics, Nanyang Technological University 637371, Singapore*
[3]*Nonlinear Physics Centre, Research School of Physics and Engineering, The Australian National University, Canberra ACT 0200, Australia*
[4]*Institute of Condensed Matter Theory and Solid State Optics, Abbe Center of Photonics, Friedrich-Schiller-Universität Jena, Jena 07743, Germany*

(Received 15 October 2013; revised manuscript received 22 August 2014; published 5 September 2014)

We consider a quantum well embedded in a zero-dimensional microcavity with a subwavelength grated mirror, where the x-linearly polarized exciton mode is strongly coupled to the cavity photon, while y-polarized excitons remain in the weak-coupling regime. Under incoherent optical or electric pumping, we demonstrate polariton bistability associated with parametric scattering processes. Such bistability is useful for constructing polaritonic devices with optical or electrical incoherent pumping.

DOI: 10.1103/PhysRevB.90.125407 PACS number(s): 78.67.−n, 42.79.Hp, 71.35.−y, 71.36.+c

I. INTRODUCTION

Bistability and hysteresis are fundamental properties of resonant optical nonlinear systems with applications in optical memory elements and transistors. Optical nonlinearity ultimately relies on the coupling of light to electronic degrees of freedom, which mediate effective interactions between photons. With an ever-growing effort devoted to the enhancement of light-matter coupling, high nonlinearity allows bistability to be routinely observed in a variety of systems.

One example is the strong light-matter coupling in high-quality factor semiconductor microcavities containing quantum well excitons [1]. The resulting exciton-polaritons exhibit bistability, when driven resonantly and coherently [2–4], i.e., with a pumping laser tuned to the energy of the exciton-polariton quasiparticle. This allows a variety of related effects to occur, including driven superfluidity [5], the suppression of disorder [6], and the formation of various structures: spin patterns [7–9], solitons [10–12], and vortex lattices [13]. Controlled switching has been observed in multimode systems, based on the overlapping of states with different energies and wave vectors [14] or the spin degree of freedom [15–17].

The advantages of exciton-polaritons include their ultrafast velocity and strength of nonlinear interactions, which was reported to result in ultrafast switching typically in the picosecond range using low (milliwatt) power in a micrometer-sized area [17]. These characteristics are very competitive with optical switching in other systems, such as microring resonators [18], organic waveguides [19], or photonic crystals [20]. Exciton-polariton bistability also underpins schemes for photonic circuits [21], where a complete logical architecture can be constructed [22]. In addition, the sensitivity of excitons to electric fields could be exploited in hybrid electro-optic devices [23] combining both photonics and electronic interfaces. The further development of hybrid polaritonic devices requires electrically injected microcavities [24–26], recently shown to enable polariton lasing [27]. However, all of the polaritonic devices based on bistability demonstrated to date require a coherent excitation, implying that they must be coupled with a laser light that is resonant or near-resonant with the exciton-polaritons.

In this paper, we propose a mechanism of optical bistability in a semiconductor microcavity compatible with incoherent nonresonant pumping. We consider the recently developed subwavelength grating type microcavity, reported by Zhang *et al.* [28] and illustrated in Fig. 1(a). In such a cavity, light is only confined if it has a specific linear polarization (x) such that linearly polarized exciton-polaritons are formed, while a cross-linearly polarized (y) exciton mode remains uncoupled to light. We develop evolution equations for occupation numbers and correlators in this system, using a master equation approach [29] accounting for incoherent pumping and dissipation. First, we consider an optical incoherent excitation of an exciton mode, which could be polarized in the y direction so as to avoid direct excitation of exciton-polariton modes. Second, we consider the electrical injection of excitons, leading to asymmetric pumping of all three modes. In both cases, excitons undergo elastic pair scattering into upper and lower polariton states, in analogy to various intrabranch [30,31] and interbranch [32–34] processes typically studied in resonantly excited microcavities. This leads to bistable behavior of the system under certain pumping conditions, which we expect to be useful for future polaritonic devices able to work under optical and electrical incoherent pumping.

II. THE MODEL

Introducing the field operators of cavity photons $\hat{\phi}$ and excitons $\hat{\chi}$, the Hamiltonian of the system can be written as

$$\hat{\mathcal{H}} = E_C\hat{\phi}_x^\dagger\hat{\phi}_x + E_X(\hat{\chi}_x^\dagger\hat{\chi}_x + \hat{\chi}_y^\dagger\hat{\chi}_y) + V(\hat{\chi}_x^\dagger\hat{\phi}_x + \hat{\phi}_x^\dagger\hat{\chi}_x) + \alpha_1(\hat{\chi}_+^\dagger\hat{\chi}_+^\dagger\hat{\chi}_+\hat{\chi}_+ + \hat{\chi}_-^\dagger\hat{\chi}_-^\dagger\hat{\chi}_-\hat{\chi}_-) + 2\alpha_2\hat{\chi}_+^\dagger\hat{\chi}_-^\dagger\hat{\chi}_+\hat{\chi}_-, \tag{1}$$

where x, y, $+$, and $-$ subscripts denote linear, cross-linear, circular, and cross-circular polarizations, respectively. We consider spin degenerate exciton states with energy E_X and a linearly polarized cavity mode with energy E_C. The exciton-photon coupling constant V couples only x polarized states. Nonlinear interactions between excitons with parallel and antiparallel spins are described by the parameters α_1 and α_2, respectively. The circularly polarized states can be rewritten in terms of linearly polarized states, $\hat{\chi}_\pm = (\hat{\chi}_x \pm i\hat{\chi}_y)/\sqrt{2}$. Introducing lower and upper x polarized polariton states, $\hat{\phi}_x = C\hat{\psi}_L - X\hat{\psi}_U$ and $\hat{\chi}_x = X\hat{\psi}_L + C\hat{\psi}_U$, we can diagonalize the

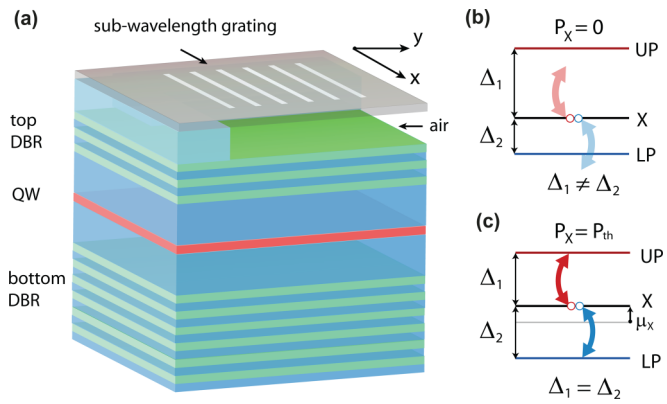

FIG. 1. (Color online) (a) Sketch of the system. The microcavity is formed from distributed Bragg reflectors (DBRs) and a subwavelength grating at the top. This allows confinement of the x-linearly polarized cavity mode only. (b) and (c) The energy levels corresponding to positive detuning. At small pumping rates of the χ_y, exciton parametric processes are not possible, since $\Delta_1 \neq \Delta_2$ (b). Above threshold pumping $P_{\rm th}$, a blueshift in the energy of χ_y satisfies the parametric scattering condition $\Delta_1 = \Delta_2$ (c).

linear part of the Hamiltonian:

$$\begin{aligned}\hat{\mathcal{H}} = {} & E_L\hat{\psi}_L^\dagger\hat{\psi}_L + E_U\hat{\psi}_U^\dagger\hat{\psi}_U + \frac{(\alpha_1+\alpha_2)}{2}(X^4\hat{\psi}_L^\dagger\hat{\psi}_L^\dagger\hat{\psi}_L\hat{\psi}_L \\ & + C^4\hat{\psi}_U^\dagger\hat{\psi}_U^\dagger\hat{\psi}_U\hat{\psi}_U + 4X^2C^2\hat{\psi}_L^\dagger\hat{\psi}_U^\dagger\hat{\psi}_L\hat{\psi}_U + \hat{\chi}_y^\dagger\hat{\chi}_y^\dagger\hat{\chi}_y\hat{\chi}_y) \\ & - (\alpha_1-\alpha_2)XC(\hat{\psi}_L^\dagger\hat{\psi}_U^\dagger\hat{\chi}_y\hat{\chi}_y + \hat{\chi}_y^\dagger\hat{\chi}_y^\dagger\hat{\psi}_L\hat{\psi}_U) \\ & + 2\alpha_1(X^2\hat{\psi}_L^\dagger\hat{\psi}_L + C^2\hat{\psi}_U^\dagger\hat{\psi}_U)\hat{\chi}_y^\dagger\hat{\chi}_y + E_X\hat{\chi}_y^\dagger\hat{\chi}_y. \end{aligned} \tag{2}$$

The polariton energies are given by $E_{U,L} = (E_C + E_X)/2 \pm \sqrt{\delta^2 + 4V^2}/2$, where $\delta = E_C - E_X$ denotes a detuning between cavity photon and exciton modes. The corresponding Hopfield coefficients X and C can be defined using relations $\{X^2, C^2\} = (1 \pm \delta/\sqrt{\delta^2+4V^2})/2$.

Given the Hamiltonian, the system evolution follows the master equation for the density matrix ρ:

$$\begin{aligned}\frac{d\rho}{dt} = {} & -\frac{i}{\hbar}[\hat{\mathcal{H}},\rho] \\ & + \sum_{a=\chi,\psi_U,\psi_L} P_a(\hat{a}\rho\hat{a}^\dagger + \hat{a}^\dagger\rho\hat{a} - \hat{a}^\dagger\hat{a}\rho - \rho\hat{a}\hat{a}^\dagger) \\ & + \sum_{a=\chi,\psi_U,\psi_L} \frac{\Gamma_a}{2\hbar}(2\hat{a}\rho\hat{a}^\dagger - \hat{a}^\dagger\hat{a}\rho - \rho\hat{a}^\dagger\hat{a}), \end{aligned} \tag{3}$$

where we defined $\hat{\chi} \equiv \hat{\chi}_y$, P_i $(i = X,L,U)$ are the rates of incoherent pumping [35,36] for different modes, and we accounted for different decay rates Γ_X, $\Gamma_U = X^2\Gamma_C + C^2\Gamma_X$, and $\Gamma_L = C^2\Gamma_C + X^2\Gamma_X$, corresponding to χ, ψ_U, and ψ_L modes. Γ_C denotes the cavity photon linewidth. We will consider two cases: (1) incoherent optical polarized pump $(P_X > 0, P_{L,U} = 0)$, where only χ_y excitons are pumped, and (2) electrical pump $(P_{X,L,U} > 0)$, where all three modes are asymmetrically populated. The density matrix allows the calculation of observable quantities such as $\langle\hat{\mathcal{O}}\rangle = \mathrm{tr}\{\hat{\mathcal{O}}\rho\}$. From Eq. (3), we can thus derive a set of equations for the population numbers of polaritons $N_{L,U} = \langle\hat{\psi}_{L,U}^\dagger\hat{\psi}_{L,U}\rangle$ and excitons $N_X = \langle\hat{\chi}^\dagger\hat{\chi}\rangle$ (see Ref. [37]):

$$\frac{dN_L}{dt} = -\frac{2\alpha_-}{\hbar}XC\Im m\{A\} - \frac{\Gamma_L}{\hbar}N_L + P_L, \tag{4}$$

$$\frac{dN_U}{dt} = -\frac{2\alpha_-}{\hbar}XC\Im m\{A\} - \frac{\Gamma_U}{\hbar}N_U + P_U, \tag{5}$$

$$\frac{dN_X}{dt} = \frac{4\alpha_-}{\hbar}XC\Im m\{A\} - \frac{\Gamma_X}{\hbar}N_X + P_X, \tag{6}$$

where $\alpha_\pm = \alpha_1 \pm \alpha_2$, the correlator $A = \langle\hat{\psi}_L^\dagger\hat{\psi}_U^\dagger\hat{\chi}\hat{\chi}\rangle$, and we used bosonic commutation rules to evaluate the commutators in Eq. (3). By truncating third-order correlators as products of lower order correlators [29] (e.g., $\langle\hat{\psi}_L^\dagger\hat{\psi}_L^\dagger\hat{\psi}_L\hat{\psi}_U^\dagger\hat{\chi}\hat{\chi}\rangle \approx \langle\hat{\psi}_L^\dagger\hat{\psi}_U^\dagger\hat{\chi}\hat{\chi}\rangle\langle\hat{\psi}_L^\dagger\hat{\psi}_L\rangle = AN_L$), the evolution equation for A is

$$\frac{dA}{dt} = \frac{i}{\hbar}(\beta_1 A + \beta_2) - \frac{\Gamma}{\hbar}A, \tag{7}$$

where $\Gamma = (\Gamma_L + \Gamma_U)/2 + \Gamma_X$, and we defined the auxiliary functions $\beta_1(N_{U,L,X})$ and $\beta_2(N_{U,L,X}^3)$, which read

$$\begin{aligned}\beta_1 = {} & \delta + \alpha_+(2X^2C^2 - 1) \\ & - 2(\alpha_+ + \alpha_-)(X^2N_L + C^2N_U) - (\alpha_+ - \alpha_-)N_X \\ & + \alpha_+[N_L(X^4 + 2X^2C^2) + N_U(C^4 + 2X^2C^2)], \\ \beta_2 = {} & \alpha_- XC\big[2N_LN_U(2N_X + 1) - (N_L + N_U + 1)N_X^2\big]. \end{aligned} \tag{8}$$

The chosen truncation of correlators, which we use to derive equations of motion, is well justified when the parametric scattering processes are accounted for [38]. In particular, it was shown that higher order correlators play a minor role for description of a system with parametric interaction [39].

Steady-state solutions can be found by setting $dN_{U,L,X}/dt = 0$ and $dA/dt = 0$. Separating the real and imaginary parts of A, gives $\Im m\{A\} = \beta_2\Gamma/(\beta_1^2 + \Gamma^2)$. The remaining equations can be reduced to a third-order equation for N_L:

$$N_L\Gamma_L(\beta_1^2 + \Gamma^2) + 2\alpha_- XC\beta_2\Gamma - \hbar P_L(\beta_1^2 + \Gamma^2) = 0, \tag{9}$$

where β_1 and β_2 can be rewritten in terms of N_L using

$$N_U = N_L\frac{\Gamma_L}{\Gamma_U} + \frac{\hbar(P_U - P_L)}{\Gamma_U}, \tag{10}$$

$$N_X = -2N_L\frac{\Gamma_L}{\Gamma_X} + \frac{\hbar(P_X + 2P_L)}{\Gamma_X}. \tag{11}$$

We note that the characteristic energy scale of the system is defined by the Rabi splitting $\Omega_R \equiv 2V$. In particular, the important parameter governing the system behavior is the ratio of the detuning to the Rabi energy, $\delta/2V$.

Since β_2 has a cubic dependence on occupation numbers, there are in general three solutions to Eq. (9). Here, we shall be interested only in real and non-negative solutions, which for certain parameters can represent bistable behavior of the system. While an analytical solution of Eq. (9) is possible, the resulting expression is too bulky to be presented here. In what follows, we present a numerical treatment of the problem only.

We restrict our treatment to a micropillar structure of small radius, which can be considered as a zero-dimensional photonic structure [40,41]. This allows us to disregard spatial dynamics in the system, leading to the simplified three-level scheme described above and shown in Fig. 1(b). Consequently, exact frequency matching is required to start populating polariton modes. For larger structures, where states with nonzero wave vectors appear, the parametric scattering conditions can change, with subsequent modification of $N_{L,U,X}$ solutions (see Ref. [37] for details).

III. INCOHERENT BISTABILITY WITH POLARIZED OPTICAL PUMP

First, we consider excitation with a broad LED beam, representing an incoherent source that is linearly polarized in the y direction using a polarizer. This excitation populates only the weakly coupled excitonic mode χ_y ($P_{L,U} = 0$). The system depends strongly on the mode detuning δ. For positive detuning and weak pump, the condition of parametric scattering between exciton and polariton modes is not satisfied [Fig. 1(b)]. However, the increase of exciton concentration with P_X leads to a blueshift of the mode, μ_X, and at a threshold intensity (estimated as $P_{th} = \delta\Gamma_X/2\hbar\alpha_+$) the energy difference between modes becomes equal and parametric scattering is possible [Fig. 1(c)]. This conversion of two y-polarized excitons into upper and lower polaritons starts to populate otherwise empty polariton modes.

The results of calculations are shown in Fig. 2 for experimentally reported parameters [28]: $V = 6$ meV, $\Gamma_C = \hbar/\tau_C$ (where $\tau_C = 5$ ps is the cavity photon lifetime), $\tau_X = 100$ ps [42], and $S = 25\ \mu\text{m}^2$ is the pump area. The exciton-exciton scattering strength in the triplet channel was calculated as $\alpha_1 = 6E_B a_B^2/S$ [43], where $E_B = 4.8$ meV and $a_B = 11.6$ nm are the exciton binding energy and Bohr radius in GaAs, respectively. α_2 was shown to vary in a broad range with varying detuning [44], or can be tuned by other means. Here, we use the value $\alpha_2 = 0.4\alpha_1$ reported in Ref. [45].

For a fixed detuning, Fig. 2(a) shows that at very low pump intensity parametric scattering does not take place, and the polariton population is zero. With increasing intensity parametric scattering is turned on, increasing the polariton population at the expense of limiting the exciton population [Fig. 2(c)]. At high pump powers, the unequal blueshifts of the modes in the system switch the parametric scattering off, with the polariton population returning to small values close to zero. A similar effect was seen in Ref. [4] in resonantly excited parametric oscillators. Here, the lower density branch has a vanishingly small occupation compared to the higher branch or excitonic mode occupancies. While being typically less than unity for small detuning, it can reach an order of one in the higher detuning region. This may not be sufficient for parametric scattering as the occupation of N_U may be suppressed at the same detuning. However, one can still expect energy relaxation mechanisms involving higher energy states [46], which can potentially lead to polariton lasing in the micropillar structure [47]. For a clear demonstration of bistability, we choose parameters where parametric scattering is dominant or the occupancy of N_L is too small for polariton lasing.

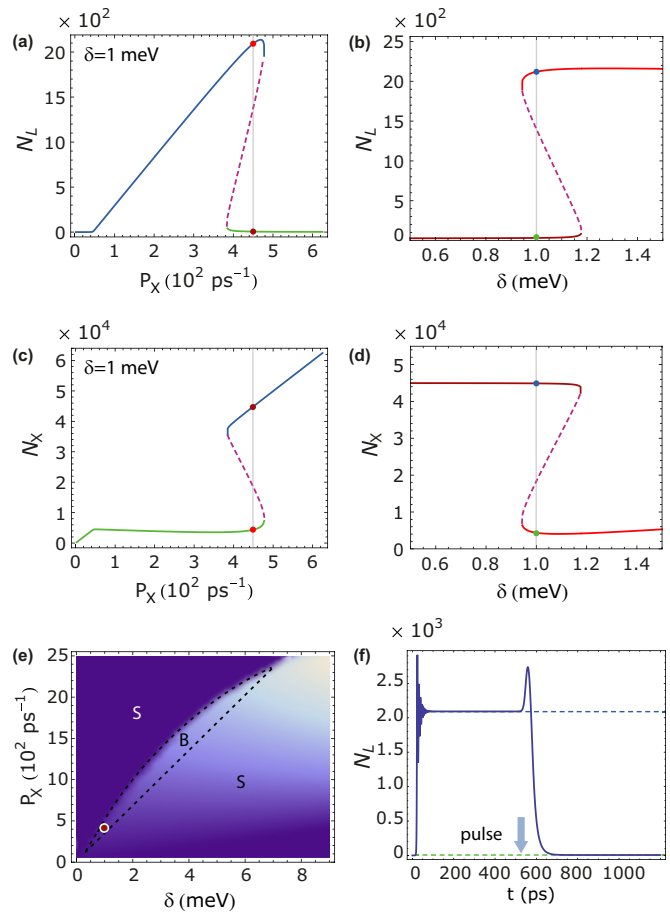

FIG. 2. (Color online) Steady-state solutions in a subwavelength grating microcavity from the analytic solution of Eqs. (9)–(11). (a) Polariton population pump power dependence (fixed $\delta = 1$ meV). The vertical gray line shows a selected pump power at which switching can be observed between the two stable states marked by spots. (b) Polariton dependence on δ [the pump power is the same as that marked by the vertical gray line in (a)]. (c) and (d) Variation of the exciton densities, corresponding to (a) and (b). (e) Phase diagram of the system in the P_X/δ coordinate plane. The intensity of the plot corresponds to the population of the highest available polariton state. The dashed curve denotes the bistable region (B), while the region (S) supports only a single solution. (f) Time dynamic simulation for the red point in (e) from the numerical extrapolation of Eqs. (4)–(7) using the Gragg-Bulirsch-Stoer algorithm. The addition of a pulse to the *cw* pump at $t = 550$ ps induces switching between the high- and low-density states marked in (a) and (b).

Due to the concurrent bistability shown by the vertical gray line in Fig. 2, the system can exist in a high or low polariton density state. Note that while the excitonic mode shows conventional S-shape bistability, the shape of lower polariton bistability is different. This can be explained keeping in mind the relations between modes given by Eq. (11). Additionally, the switching between high- and low-density states can be controlled with detuning between modes, as shown in Figs. 2(b) and 2(d).

The system is further characterized by the phase diagram in the P_X/δ plane shown in Fig. 2(e). The dashed boundary marks the region in which multiple solutions are present. Taking

parameters at the red dot in Fig. 2(e), switching between stable states can be demonstrated by numerical solution of Eqs. (4)–(7), as shown in Fig. 2(f). Assuming that the system is initially unoccupied, by switching on the continuous wave (*cw*) pump, the system is quickly stabilized into the higher polariton density state shown in Figs. 2(a)–2(d). A short pulse applied at $t = 550$ ps is able to switch the system into the lower density state. During the intervals without pulses, the system is stable, remaining in the state set by its history. We note that the appearance of the bistability window also depends on the singlet interaction constant α_2, favoring small $\alpha_- = \alpha_1 - \alpha_2$.

In order to give an intuitive explanation of the observed bistability effect, we can rewrite Eq. (7) in the form

$$i\hbar\frac{dA}{dt} = [-\delta + \widetilde{\mu}(A) - i\Gamma]\,A + \widetilde{P}, \tag{12}$$

where we defined the effective energy shift $\widetilde{\mu}(A) = -\beta_1 + \delta$ and effective pumping amplitude at zero frequency $\widetilde{P} = -\beta_2$. We expect the bistable window to coincide with the resonance point in Eq. (12) where the amplitude of A can become strongly enhanced. This corresponds to a situation where the nonlinear term (blueshift $\widetilde{\mu}$) brings the system into resonance with the effective "coherent" pump of the correlator A. This occurs when $\beta_1 \approx 0$ and was verified numerically by tracking the sign of β_1.

Previously, we restricted our consideration to the purely zero-dimensional case, where both polaritonic and excitonic modes can be described by a three-level system. However, while the confinement of polaritonic modes is fully justified in the case of a microcavity with subwavelength grating [28], the free excitons can still possess spatial dynamics. We have also considered the exciton dispersion (Ref. [37], second section), and have shown that it does not qualitatively change the described incoherent bistability.

While we did not consider thermal/quantum noise, calculations for resonant excitation suggest only a slight narrowing of the hysteresis cycle [48]. Despite fluctuations, resonant experiments show very long memory times [17].

IV. INCOHERENT BISTABILITY WITH ELECTRICAL PUMP

Next, we consider the case of electrical injection of excitons, where both x- and y-polarized excitonic modes are pumped ($P_{L,U} \neq 0$). The dependence of the lower polariton occupation number N_L on pumping strength P_X is shown in Fig. 3(a) and reveals electrically pumped bistability. The key difference between electrical pumping and the optical polarized pump considered above is additional excitation of polariton modes with rates P_L for lower polaritons and P_U for upper polaritons, which are different in the case of nonzero detuning and due to presence of thermalization processes. Particularly, the upper polariton mode occupation is typically small, while relaxation mechanisms lead to effective incoherent pumping of lower polariton modes. This leads to an asymmetric blue shift of both exciton and polariton energies, and consequent shift of $P_{\rm th}$ to higher pumping rates. Additionally, an incoherent bistability with electrical

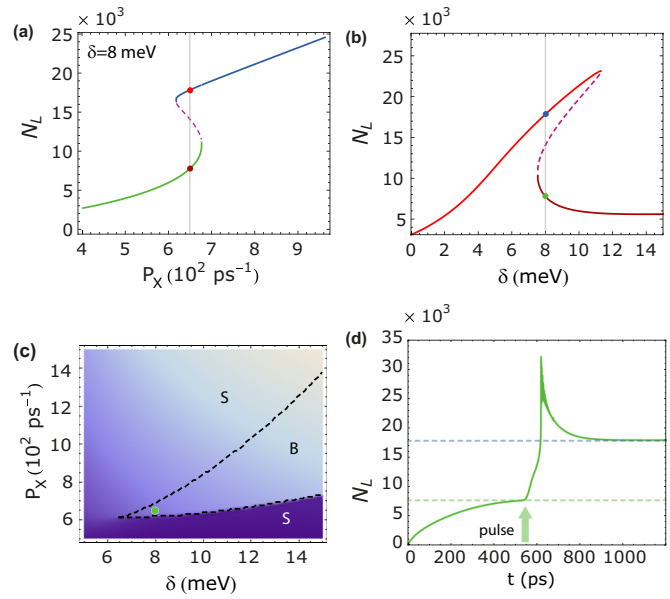

FIG. 3. (Color online) Steady-state solutions in a subwavelength grating microcavity with electrical pumping from Eqs. (9)–(11). (a) Dependence of the lower polariton N_L population on pumping strength P_X plotted for detuning $\delta = 8$ meV. (b) Lower polariton population shown as a function of detuning for fixed pump $P_X = 6.5 \times 10^2$ ps^{-1}. (c) Phase diagram plotted in P_X/δ marking bistable (B) and single solution (S) regions. (d) Simulation of the lower polariton occupation number as a function of time [using Eqs. (4)–(7)], showing switching between low- and high-intensity states (dashed lines). An additional pulse arrives at $t = 550$ ps. Parameters are shown by the green dot in (c).

injection requires larger positive detuning than that with optical pumping and negative α_2 [see Fig. 3(b)]. Large, positive values of detuning are accessible in current experiments [49,50].

The phase diagram in the P_X/δ plane is shown in Fig. 3(c). One can see that the range of the pumping strengths corresponding to the bistability window diminishes compared to the optical case, although is still fully accessible. Finally, the switching behavior of the modes, calculated similarly to the optical pump case, confirms stability of the polariton modes with the high and low population [Fig. 3(d)]. For the calculations in Fig. 3, we considered the system with a single GaAs quantum well (QW) in the cavity, with light-matter interaction constant being $V = 2$ meV, $\alpha_2 = -0.4\alpha_1$, and effective pumping amplitudes of polariton states $P_U = 0.01C^2P_X$ and $P_L = 0.1X^2P_X$.

Finally, in order to show the possible window of parameters hosting the bistability effects, we perform calculations for systems with different nonlinear interaction constant ratios α_2/α_1 and cavity photon lifetime τ_C. The results are shown in Fig. 4, where we varied parameters for the cases of optical [Figs. 4(a) and 4(c)] and electrical [Figs. 4(b) and 4(d)] pump. In the case of optical incoherent drive, the detuning was fixed to $\delta = 4$ meV, and for electrical case, it is chosen as $\delta = 8$ meV.

In both cases presented in plots (a) and (b), the increase of the bistable window favors large absolute value of the singlet interaction constant, comparing to the triplet one, $|\alpha_2/\alpha_1| >$

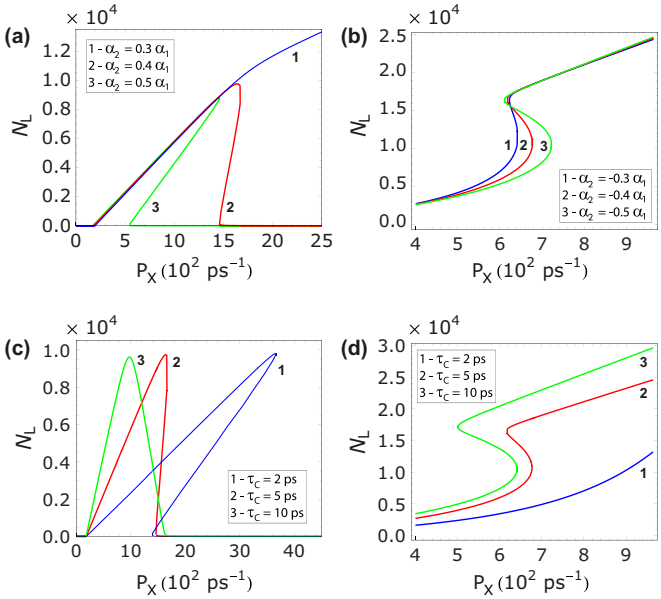

FIG. 4. (Color online) Dependence of the lower polariton population N_L as a function of optical [(a) and (c)] and electrical [(b) and (d)] incoherent pump power. Each plot shows the bistability curves for varying nonlinear interaction constant α_2 [(a) and (b)] and cavity photon lifetime τ_C [(c) and (d)].

0.4. Thus, for an experimental realization of the described effects, one should search for the system with a pronounced spin dependence of nonlinear polariton interaction.

The dependence of incoherent bistability on the cavity photon lifetime is shown in Figs. 4(c) and 4(d) for optical and electrical pumps, respectively. In the case of optical pump, the behavior is rather unexpected, showing that appearance of the bistable window is favored in the low-Q cavity limit (while keeping the strong coupling regime). For the electrical pumping case, the dependence is conventional, meaning that the bistable window grows with the photon lifetime.

V. CONCLUSIONS

We considered parametric scattering between y polarized excitons and x polarized polaritons in a subwavelength grating microcavity. We demonstrated bistable behavior in the cases of both incoherent optical polarized pumping and electrical exciton excitation. This theoretical evidence for fast-response off-resonantly driven bistability lays a foundation for hybrid electro-optic polaritonic devices.

ACKNOWLEDGMENTS

I.A.S. acknowledges support from the FP7 IRSES project POLAPHEN and Tier 1 project "Polaritons for novel device applications." O.A.E. acknowledges support from the DFG project EG 344/2-1 and the TMESC project B514-11027. E.A.O. acknowledges support from the Australian Research Council. O.K. acknowledges support from the Eimskip Fund.

[1] A. V. Kavokin, J. J. Baumberg, G. Malpuech, and F. P. Laussy, *Microcavities* (Oxford University Press, New York, 2007).
[2] N. A. Gippius, S. G. Tikhodeev, V. D. Kulakovskii, D. N. Krizhanovskii, and A. I. Tartakovskii, Europhys. Lett. **67**, 997 (2004).
[3] A. Baas, J. P. Karr, H. Eleuch, and E. Giacobino, Phys. Rev. A **69**, 023809 (2004).
[4] D. M. Whittaker, Phys. Rev. B **71**, 115301 (2005).
[5] I. Carusotto and C. Ciuti, Phys. Rev. Lett. **93**, 166401 (2004).
[6] T. C. H. Liew, Phys. Stat. Sol. (b) **249**, 880 (2012).
[7] I. A. Shelykh, T. C. H. Liew, and A. V. Kavokin, Phys. Rev. Lett. **100**, 116401 (2008).
[8] D. Sarkar, S. S. Gavrilov, M. Sich, J. H. Quilter, R. A. Bradley, N. A. Gippius, K. Guda, V. D. Kulakovskii, M. S. Skolnick, and D. N. Krizhanovskii, Phys. Rev. Lett. **105**, 216402 (2010).
[9] C. Adrados, A. Amo, T. C. H. Liew, R. Hivet, R. Houdré, E. Giacobino, A. V. Kavokin, and A. Bramati, Phys. Rev. Lett. **105**, 216403 (2010).
[10] Y. Larionova, W. Stolz, and C. O. Weiss, Optics Lett. **33**, 321 (2008).
[11] O. A. Egorov, D. V. Skryabin, A. V. Yulin, and F. Lederer, Phys. Rev. Lett. **102**, 153904 (2009); O. A. Egorov, A. V. Gorbach, F. Lederer, and D. V. Skryabin, *ibid.* **105**, 073903 (2010); O. A. Egorov and F. Lederer, Phys. Rev. B **87**, 115315 (2013).
[12] M. Sich, D. N. Krizhanovskii, M. S. Skolnick, A. V. Gorbach, R. Hartley, D. V. Skryabin, E. A. Cerda-Méndez, K. Biermann, R. Hey, and P. V. Santos, Nat. Photon. **6**, 50 (2012).
[13] A. V. Gorbach, R. Hartley, and D. V. Skryabin, Phys. Rev. Lett. **104**, 213903 (2010).
[14] M. De Giorgi *et al.*, Phys. Rev. Lett. **109**, 266407 (2012).
[15] A. Amo, T. C. H. Liew, C. Adrados, R. Houdré, E. Giacobino, A. V. Kavokin, and A. Bramati, Nat. Photon. **4**, 361 (2010).
[16] C. Adrados, T. C. H. Liew, A. Amo, M. D. Martín, D. Sanvitto, C. Antón, E. Giacobino, A. Kavokin, A. Bramati, and L. Viña, Phys. Rev. Lett. **107**, 146402 (2011).
[17] R. Cerna, Y. Léger, T. K. Paraïso, M. Wouters, F. Morier-Genoud, M. T. Portella-Oberli, and B. Deveaud, Nat. Commun. **4**, 2008 (2013).
[18] M. Waldow *et al.*, Opt. Express. **16**, 7693 (2008).
[19] C. Koos *et al.*, Nat. Photon. **3**, 216 (2009).
[20] K. Nozaki *et al.*, Nat. Photon. **4**, 477 (2010).
[21] D. Ballarini, M. De Giorgi, E. Cancellieri, R. Houdré, E. Giacobino, R. Cingolani, A. Bramati, G. Gigli, and D. Sanvitto, Nat. Commun. **4**, 1778 (2013).
[22] T. Espinosa-Ortega and T. C. H. Liew, Phys. Rev. B **87**, 195305 (2013).
[23] T. C. H. Liew, A. V. Kavokin, T. Ostatnický, M. Kaliteevski, I. A. Shelykh, and R. A. Abram, Phys. Rev. B **82**, 033302 (2010).

[24] S. I. Tsintzos, N. T. Pelekanos, G. Konstantinidis, Z. Hatzopoulos, and P. G. Savvidis, Nature (London) **453**, 372 (2008); S. I. Tsintzos, P. G. Savvidis, G. Deligeorgis, Z. Hatzopoulos, and N. T. Pelekanos, Appl. Phys. Lett. **94**, 071109 (2009).
[25] R. Butte and N. Grandjean, Semicond. Sci. Technol. **26**, 014030 (2011).
[26] K. Winkler, C. Schneider, J. Fischer, A. Rahimi-Iman, M. Amthor, A. Forchel, S. Reitzenstein, S. Höfling, and M. Kamp, Appl. Phys. Lett. **102**, 041101 (2013).
[27] C. Schneider *et al.*, Nature (London) **497**, 348 (2013).
[28] B. Zhang, Z. Wang, S. Brodbeck, C. Schneider, M. Kamp, S. Höfling, and H. Deng, Light: Sci. Appl. **3**, e135 (2014).
[29] I. A. Shelykh, L. Viña, A. V. Kavokin, N. G. Galkin, G. Malpuech, and R. André, Solid State Commun. **135**, 1 (2005).
[30] P. G. Savvidis, J. J. Baumberg, R. M. Stevenson, M. S. Skolnick, D. M. Whittaker, and J. S. Roberts, Phys. Rev. Lett. **84**, 1547 (2000); A. I. Tartakovskii, D. N. Krizhanovskii, and V. D. Kulakovskii, Phys. Rev. B **62**, R13298(R) (2000).
[31] S. Savasta, O. Di Stefano, V. Savona, and W. Langbein, Phys. Rev. Lett. **94**, 246401 (2005).
[32] C. Ciuti, Phys. Rev. B **69**, 245304 (2004).
[33] C. Diederichs, J. Tignon, G. Dasbach, C. Ciuti, A. Lemaître, J. Bloch, P. Roussignol, and C. Delalande, Nature (London) **440**, 904 (2006).
[34] W. Xie, H. Dong, S. Zhang, L. Sun, W. Zhou, Y. Ling, J. Lu, X. Shen, and Z. Chen, Phys. Rev. Lett. **108**, 166401 (2012).
[35] F. P. Laussy, E. del Valle, and C. Tejedor, Phys. Rev. Lett. **101**, 083601 (2008).
[36] E. del Valle and F. P. Laussy, Phys. Rev. Lett. **105**, 233601 (2010).
[37] See Supplemental Material at http://link.aps.org/supplemental/10.1103/PhysRevB.90.125407 for the derivation of equations for occupation numbers and correlators, and accounting of the spatial dynamics in the system.
[38] T. C. H. Liew and V. Savona, Phys. Rev. A **84**, 032301 (2011).
[39] K. Kristinsson, O. Kyriienko, T. C. H. Liew, and I. A. Shelykh, Phys. Rev. B **88**, 245303 (2013).
[40] L. Ferrier, S. Pigeon, E. Wertz, M. Bamba, P. Senellart, I. Sagnes, A. Lematre, C. Ciuti, and J. Bloch, Appl. Phys. Lett. **97**, 031105 (2010).
[41] L. Ferrier, E. Wertz, R. Johne, D. D. Solnyshkov, P. Senellart, I. Sagnes, A. Lemaître, G. Malpuech, and J. Bloch, Phys. Rev. Lett. **106**, 126401 (2011).
[42] B. Sermage, S. Long, I. Abram, J. Y. Marzin, J. Bloch, R. Planel, and V. Thierry-Mieg, Phys. Rev. B **53**, 16516 (1996).
[43] F. Tassone and Y. Yamamoto, Phys. Rev. B **59**, 10830 (1999).
[44] M. Vladimirova, S. Cronenberger, D. Scalbert, K. V. Kavokin, A. Miard, A. Lemaître, J. Bloch, D. Solnyshkov, G. Malpuech, and A. V. Kavokin, Phys. Rev. B **82**, 075301 (2010).
[45] T. K. Paraïso, M. Wouters, Y. Léger, F. Mourier-Genoud, and B. Deveaud-Plédran, Nat. Mater. **9**, 655 (2010).
[46] D. Porras, C. Ciuti, J. J. Baumberg, and C. Tejedor, Phys. Rev. B **66**, 085304 (2002).
[47] D. Bajoni, P. Senellart, E. Wertz, I. Sagnes, A. Miard, A. Lemaître, and J. Bloch, Phys. Rev. Lett. **100**, 047401 (2008).
[48] R. Johne, N. S. Maslova, and N. Gippius, Solid State Commun. **149**, 496 (2009).
[49] Feng Li *et al.*, Phys. Rev. Lett. **110**, 196406 (2013).
[50] A. Trichet, E. Durupt, F. Médard, S. Datta, A. Minguzzi, and M. Richard, Phys. Rev. B **88**, 121407(R) (2013).